Crumbs3 is expressed in oral squamous cell carcinomas and promotes cell migration and proliferation by affecting RhoA activity

YUSUKE YOKOYAMA[1,2], HIDEKAZU IIOKA[1], ARATA HORII[2] and EISAKU KONDO[1,3]

[1]Division of Molecular and Cellular Pathology, [2]Department of Otolaryngology, Head and Neck Surgery, Niigata University Graduate School of Medical and Dental Sciences, Niigata 951-8510; [3]Division of Tumor Pathology, Near InfraRed Photo-ImmunoTherapy Research Institute, Kansai Medical University, Hirakata, Osaka 573-1010, Japan

Received November 25, 2021; Accepted March 17, 2022

DOI: 10.3892/ol.2022.13293

Abstract. Despite the recent progression of treatments, the 5-year survival rate of patients with oral squamous cell carcinoma (OSCC) is still poor. One of the most critical factors affecting prognosis is tumor metastasis. Developing novel molecular targeted therapies by analyzing the molecular pathway of OSCC metastasis is an urgent issue. The present study aimed to characterize the expression and function of crumbs3 (Crb3) in OSCC cell migration. Immunohistochemistry and immunoblotting revealed that Crb3 was expressed in tissues from patients with OSCC and OSCC cell lines. The motility of OSCC cell lines was decreased by knockdown of *Crb3* without affecting proliferation. However, *Crb3*-knockout (KO) clones exhibited decreases in both cell migration and proliferation. The expression of epithelial-mesenchymal transition markers was not altered in *Crb3*-KO clones compared with parent cells. A xenograft mouse model of lung metastasis revealed that the metastatic potential of *Crb3*-KO clones was reduced. As seen with *Crb3*-KO clones, the motility of OSCC cells was decreased by treatment with inhibitors of RhoA activation. Serum-induced activation of RhoA in OSCC cells was evaluated by comparing the amount of GTP-bound RhoA using affinity matrices, revealing that RhoA activation was decreased in *Crb3*-KO clones. To the best of our knowledge, the present study was the first to demonstrate that Crb3 was expressed in squamous cell carcinoma tissues and promoted cell migration and proliferation, which was associated with RhoA activation in OSCC cells.

Correspondence to: Dr Hidekazu Iioka or Professor Eisaku Kondo, Division of Molecular and Cellular Pathology, Niigata University Graduate School of Medical and Dental Sciences, 1-757 Asahimachi-dori, Chuo-ku, Niigata 951-8510, Japan
E-mail: hiioka@med.niigata-u.ac.jp
E-mail: ekondo@med.niigata-u.ac.jp

Abbreviations: Crb3, crumbs3; HNSCC, head and neck squamous cell carcinoma; OSCC, oral squamous cell carcinoma

Key words: crumbs, Crb3, HNSCC, OSCC, squamous cell carcinoma, ras homolog family member A, metastasis

Introduction

Head and neck carcinoma is the seventh most common cancer by worldwide incidence (1). Cancers of this type develop in the craniocervical region, including the oral cavity, nasal cavity, pharynx, and larynx. Approximately 90% of lesions are histopathologically diagnosed as head and neck squamous cell carcinoma (HNSCC) (1,2). In recent decades, HNSCC treatments such as surgical and radiotherapeutic techniques, along with combined modality therapies, have improved remarkably, and disease-free survival of patients has been dramatically extended. However, the five-year survival rate of patients with HNSCC has remained 50-60% with no significant change, in part because of tumor cell invasion followed by metastasis (3,4). The largest studies have reported that the incidence of distant metastases in HNSCC patients is approximately 3% at initial presentation (5,6). However, distant metastasis during the course of the disease varies between 9 and 38% (7-9). Autopsy studies have revealed an even higher incidence of distant metastasis (10,11). Overall survival at 24 months after diagnosis of distant metastases is only 4-26.2% (12,13), and the median time from distant metastasis to death is only 3.3-10 months (12-14). Thus, epidemiological data indicate that the control of invasion and metastasis is an urgent issue for therapy of HNSCC.

Rho-family GTPases are small guanine nucleotide-binding proteins (G-proteins) that serve as critical regulators of cell adhesion, migration, and spreading, exerting their effects by modulating cytoskeletal dynamics through downstream effector proteins (15). The activity of small G-proteins is switched by guanine-nucleotide binding. The GTP-bound form activates effector proteins. However, when GTP is cleaved, the protein transitions to a GDP-bound form that cannot activate effectors. Guanine nucleotide exchange factors (GEFs)

facilitate the exchange of GDP to GTP on small G-proteins, while GTPase-activating proteins (GAPs) and GDP dissociation inhibitors (GDIs) negatively regulate the activity of small G-proteins. Another factor affecting the activity of Rho-family GTPases is phosphorylation. Phosphorylation at Ser-188 on RhoA by cAMP/cGMP-dependent kinase negatively regulates RhoA activity by enhancing interaction with GDI (16). The correlation between expression or activation of Rho-family GTPases and tumor progression is context dependent. However, RhoA is overexpressed in 80% of HNSCCs compared with adjacent non-neoplastic epithelial tissues (17). In addition, cortactin-dependent expression and activation of RhoA has been shown to promote cell cycle progression in the hypopharyngeal squamous cell carcinoma cell line FaDu (18). Similarly, activation and serine-phosphorylation of RhoA are associated with cell motility and invasion under the regulation of protein kinase C (PKC) ε in UMSCC11A and UMSCC36 cell lines (19). Epidermal growth factor receptor (EGFR) and the hyaluronan receptor CD44 are known to form a complex that promotes growth and cell migration via leukemia-associated RhoGEF (LARG), a RhoA specific GEF, in the HNSCC cell line HSC-3 (20). Vav guanine nucleotide exchange factor 2 (VAV2) is another Rho-specific GEF that is overexpressed in HNSCCs and has been shown to associate with regenerative proliferation in a RhoA-dependent manner (21). Considered together, these findings support the hypothesis that activation of RhoA promotes HNSCC progression.

Crumbs (Crb)-family single-transmembrane proteins are expressed in normal epithelial tissues, where Crb molecules contribute to the establishment of apicobasal cell polarity. The mammalian crumbs3 (Crb3) protein is a homolog of the *Drosophila* Crb protein, and *Crb3* seems to be expressed in epithelial tissues (22). *Crb3*-knockout (KO) mice show defects in the formation of glandular epithelium in lung, kidney, and colon tissues (23,24). The expression and function of Crb3 in normal squamous epithelium (including skin, esophagus, and oral tissues) have not (to our knowledge) been examined. Our recent study demonstrated that Crb3 is strongly expressed in colon adenocarcinomas, especially in metastatic foci, in comparison with non-neoplastic colon epithelium, where the protein promotes invasion and metastasis by activating fibroblast growth factor receptor (FGFR) signaling (25). However, the expression and function of Crb3 in other carcinomas remains poorly elucidated. In the present study, we revealed that Crb3 is endogenously expressed in HNSCC tissues. HNSCC consists of heterogeneous subgroups that arise from the oral cavity, larynx, oropharynx, and hypopharynx. Oral squamous cell carcinoma (OSCC) is the largest subgroup that constitutes approximately 40% of all HNSCC. Functional analyses of Crb3 were performed by either knock-down or knock-out of *Crb3* in OSCC cell lines. Our results suggested that Crb3 is expressed in OSCC cell lines and promotes cell migration. To investigate how Crb3 regulates the motility of OSCC cells, the activity of RhoA was evaluated. A RhoA activation assay revealed that the GTP-bound form of RhoA is significantly depleted in *Crb3*-KO OSCC cell lines. This result represents the first evidence that Crb3 promotes cell migration and RhoA activation in squamous cell carcinomas.

Materials and methods

Cell lines. Human OSCC cell lines Ca9-22, HSC-2, and HSC-3 were obtained from the JCRB (Japanese Collection of Research Bioresources) Cell Bank. The primary normal human dermal fibroblast (NHDF) cell was obtained from ATCC (#PCS-201-012, American Type Culture Collection). *Crb3*-KO derivatives of OSCC cell lines were created by targeting a genomic sequence (CCGTTCCTGCTGGCCCGCTG) in the *Crb3* allele using CRISPR-Cas9-based technology (25). The isolation of single-cell clones of *Crb3*-KO cells was performed by serial dilution. Deficiency of Crb3 protein was confirmed by immunoblotting. All cell lines were cultured in RPMI-1640 medium (#189-02025, FUJIFILM Wako Chemicals) supplemented with 10~15% fetal bovine serum (FBS) (Hyclone, #SH30071, Cytiva) and Penicillin-Streptomycin Solution (#168-23191, FUJIFILM Wako Chemicals) at 37˚C in a humidified 5% CO_2 incubator. All the OSCC cell lines used in this study were authenticated by STR analysis employing the GenePrint 10 System (Promega) as shown in a previous project (26) The patterns of STR markers of Ca9-22, HSC-2, and HSC-3 used in this study were 100% identical with JCRB0625 (Ca9-22), JCRB0622 (HSC-2), and JCRB0623 (HSC-3), respectively.

Immunohistochemistry and absorption test. Immunohistological experiments using tumor tissues surgically obtained from patients with HNSCC were approved by the Research Ethics Committee of Niigata University (approval no. 2019-0101). The patients >20 years old who were diagnosed with HNSCC by two pathologists and underwent radical surgical treatment at the Niigata University Hospital from April 1, 2017 to March 31, 2019 were included. All participants provided informed consent to participate in this study. The patient who refused to participate in the study were excluded. A total of fourteen cases of primary OSCC tissue (5 cases from tongue, 3 cases from oral floor, 3 cases from pharynx, 2 cases from larynx, and 1 case from gingiva) and 3 cases of paired cervical lymph node metastatic lesions from consecutive patients were analyzed. TNM staging was determined according to the 8th edition of the Union for International Cancer Control TNM classification. For the immunohistochemistry, paraffin-embedded sections were deparaffinized, and antigen retrieval was performed in 10 mM sodium citrate buffer (pH 6.0) using a Pascal Pressure Chamber. Antigen-retrieved sections were incubated overnight at 4˚C with anti-human Crb3 monoclonal antibody in phosphate-buffered saline (PBS) containing 1% bovine serum albumin (BSA), then stained using a Histofine DAB (diaminobenzidine) substrate kit (#425011, Nichirei Bioscience). The anti-human Crb3 monoclonal antibody (anti-Crb3 antibody) was obtained as described previously (25). The DAB-stained sections were counterstained with Mayer's hematoxylin (#30004, Mutoh Pure Chemical Industries). For the absorption test, 2.0 μg of anti-Crb3 antibody and 0.75 μg of the epitope peptide (NH2-VGARVPPTPNLKLPPEERLI, 1:25 molar ratio) were mixed in 1.2 ml of PBS containing 1% BSA and incubated for 15 min at room temperature before initiating the primary antibody reaction.

Immunoblotting. Commercially obtained antibodies employed in this study were as follows: anti-β-tubulin (1/2,000 dilution;

#PM054-7, Medical & Biological Laboratories), anti-RhoA (1/250 dilution; #ARH05, Cytoskeleton, Inc.), anti-SNAIL2 (1/1,000 dilution; #12129-1-AP, Proteintech), and anti-E-cadherin (1/1,000 dilution; #610181, BD Biosciences). Antibody dilutions and reactions were performed using Can Get Signal Solution 1 (#NKB-201, Toyobo). Freshly cultured cells were washed in PBS and lysed by adding 1X Laemmli sample buffer. After incubation at 95˚C for 3 min, protein samples were separated by sodium dodecyl sulfate-polyacrylamide gel electrophoresis (SDS-PAGE) using Tris-glycine buffer. For immunoblotting using Crb3 antibody, blocking of protein-bound PVDF membranes was performed using 0.2% BSA (#017-25771, FUJIFILM Wako Chemicals). For immunoblotting using anti-RhoA antibody, blocking of membranes was performed using TBST (10 mM Tris, pH 7.2, 0.05% Tween-20) containing 1% skimmed milk. For immunoblotting with all other primary antibodies, blocking of membranes was performed with PBST (PBS, 0.05% Tween-20) containing 1% skimmed milk. All blocking reactions consisted of a 30-min incubation. The reactions with horseradish peroxidase (HRP)-conjugated secondary antibody and membrane washing were conducted in PBST or TBST. Immunoreactivity was visualized using ImmunoStar® Zeta (#291-72401, FUJIFILM Wako Chemicals) or ImmunoStar® LD (#296-69901, FUJIFILM Wako Chemicals) and detected using the ChemiDoc Touch MP Imaging System (#17001402JA, Bio-Rad).

Immunofluorescence. Freshly cultured cells were fixed in 4% paraformaldehyde for 10 min at room temperature. Fixed cells were washed twice in PBS and permeabilized in PBST for 10 min at room temperature. Permeabilized cells were blocked in PBST containing 1% BSA for 30 min at room temperature. Immunoreaction with anti-Crb3 antibody or anti-RhoA antibody (1:1,000) diluted in PBS was carried out overnight at 4˚C on a reciprocal shaker. Immunoreaction of fluorescent dye-conjugated secondary antibody was performed for 30 min at room temperature. Counterstaining with Hoechst 33342 (#H-3570, Thermo Fisher Scientific) was performed simultaneously with the secondary antibody reaction. Fluorescent images were acquired using an inverted fluorescence microscope (IX71, Olympus).

Transfection of siRNA. *Crb3* gene silencing in OSCC cells was performed using Silencer Select pre-designed siRNAs (Thermo Fisher Scientific). The product number and target sequence of siRNAs used to knock-down *Crb3* were as follows: si*Crb3*-1 (#s40936, CAGGGAAGAAGGUACUUCA), si*Crb3*-2 (#s195567, AGUGCUUAAUAGCAGGGAA). Silencer select Negative Control No. 1 siRNA (#4390843, Thermo Fisher Scientific) was used as a control. siRNAs (10 nM final concentration) were transfected using ScreenFect™ siRNA (#299-75001, FUJIFILM Wako Chemicals) and a forward transfection protocol.

MTT assay. Cells ($1x10^4$ per well) were seeded into 24-well plates in RPMI-1640 medium supplemented with 10% FBS (10% FBS/RPMI-1640); plates were incubated at 37˚C in a 5% CO_2 incubator. Cell growth was assessed using MTT reagent (Cell Count Reagent SF, #07553-44, Nacalai Tesque) starting 24 h after seeding, and analysis was repeated every 24 h thereafter by measuring the absorbance at 450 nm using an iMark microplate reader (#1681135JA, Bio-Rad). To assess the effect of RhoA inhibitors, culture medium was replaced with fresh medium containing 15 μM Y16 (#Y-12649, MedChemExpress, NJ, USA) or 20 μM Rhosin (#555460, Merck, NJ, USA) at 24 h after seeding the cells.

Transwell migration assay. To evaluate cell migration ability, $1x10^5$ OSCC cells suspended in 200 μl Opti-MEM were loaded into the upper compartment of a Transwell chamber (#3422, Corning, Inc.). The lower chamber was loaded with 500 μl of Opti-MEM supplemented with 10% FBS. At 24-48 h after seeding, the cells in the upper chamber were removed with a cotton swab, and the remaining cells (those that had migrated through the Transwell membrane) were stained with Hoechst 33342. Fluorescent images were captured using an inverted fluorescence microscope (IX71). The number of nuclei was counted in three different fields using ImageJ software (version 1.52a, https://imagej.net/). To investigate whether RhoA inhibitors affect cell migration, the cells were pretreated with 10% FBS/RPMI-1640 containing 15 μM Y16 or 20 μM Rhosin for 24 h. Y16 or Rhosin was added to the growth medium in both the upper and lower chambers to ensure consistent exposure.

Xenograft model of OSCC lung metastases. All procedures were in accordance with the protocols approved by the Animal Care and Use Committee of Niigata University School of Medicine (approval number: SA00875). Six immunodeficient mice (SHO-*Prkdc*^{scid} *Hr*^{hr}) were obtained from Charles River Laboratories International, Inc.. The animals were maintained at 22-24˚C and 40-60% humidity under a light-dark (12-12 h) cycle of *ad libitum* feeding in a specific pathogen-free environment. Suspensions of wild-type or *Crb3*-KO HSC-2 cells ($1x10^6$/200 μl PBS) were injected into tail veins of 10-week-old female mice using 29-gauge insulin syringes. The average weight was 28.5 gram/mouse at the start of the experiment. Wild-type (n=3) and *Crb3*-KO (n=3) cell-injected mice were sacrificed concurrently between 61-75 days after injection. 20% of body weight reduction from baseline or the defined period of 75 days were used to determine the endpoint of the experiment. Cervical dislocation was conducted for euthanasia of mice. The animals were anesthetized by intraperitoneal injection of combination anesthetic (0.3 mg/kg of medetomidine, 4.0 mg/kg of midazolam, and 5.0 mg/kg of butorphanol) before euthanasia. Isolated lung specimens were fixed with 10% buffered formalin for 48 h and embedded in paraffin.

Detection of serum-induced activation of RhoA. Cells ($1x10^6$) were seeded in a 35-mm dish and incubated for 24 h. Cells then were washed twice with PBS and serum-starved for 2 h in Opti-MEM at 37˚C in 5% CO_2. Next, cells were stimulated for 30 min in RPMI-1640 containing 10% FBS at 37˚C in 5% CO_2. Isolation of activated RhoA protein from the cell lysate was performed using the Rho Activation Assay Biochem Kit (# BK036-S, Cytoskeleton) according to the manufacturer's instructions. The protein samples were subjected to 15% SDS-PAGE followed by immunoblot analysis using anti-RhoA-specific antibody.

Statistical analysis. The data from MTT and Transwell assays are presented as the mean ± SD of triplicate experiments. Statistical significance was determined using a one-way ANOVA followed by Bonferroni's post hoc test. BellCurve for Excel (version 3.23), a statistical add in software was purchased (https://bellcurve.jp/ex/, Social Survey Research Information Co., Ltd.) and used by adding into Microsoft Excel 2013 to conduct statistical analyses. $P<0.05$ was considered to indicate a statistically significant difference.

Results

Crb3 is expressed in HNSCC patient tissues. Immunohistochemistry was performed on formalin-fixed paraffin-embedded tissue sections from fourteen patients with HNSCC using a monoclonal anti-Crb3 antibody (Figs. 1, S1 and S2; Table SI). Absorption tests were performed in parallel to evaluate the specificity of the antibody and the level of background staining (Figs. S1 and S2). All of the primary HNSCC tissues and metastatic lesions in cervical lymph nodes showed positive staining for Crb3; the absorption tests did not detect background staining, confirming the specificity of the antibody (Figs. 1, S1 and S2). HNSCCs appeared to display stronger Crb3 staining than did adjacent non-neoplastic squamous epithelial tissues (Fig. S1). Most Crb3-positive cells were observed in the prickle cell layer, with Crb3 protein exhibiting apically distributed localization in juxtanuclear cytoplasm in non-neoplastic tissues (Fig. S1).

Crb3 is expressed in OSCC cell lines. Next, the endogenous expression of Crb3 protein in OSCC cell lines Ca9-22, HSC-2, and HSC-3 was evaluated by immunoblotting using a monoclonal anti-Crb3 antibody. Cell lysates from the colon cancer cell line DLD-1 and normal human dermal fibroblasts (NHDFs) were employed as positive and negative controls, respectively. Expression of Crb3 was detected in Ca9-22, HSC-2, and HSC-3. Although Crb3 is predicted to have a molecular mass of approximately 13 kDa, immunoblotting detected the protein as multiple smeary bands in the 25- to 45-kDa range (Fig. 2A). These data suggested that Crb3 protein is modified by N-glycosylation in OSCC cells, as had been reported in adenocarcinoma cells and MDCK cells (27,28). In addition, immunofluorescent staining of OSCC cell lines was performed. Crb3 localized primarily in cytoplasmic granules in HSC-2 and HSC-3 cells, while Ca9-22 cells showed dispersed localization of Crb3 in the cytoplasm and partly in the plasma membrane (Fig. 2B). These subcellular localization patterns of Crb3 were commonly observed in OSCC cells in patient tissues (Figs. 1, S1 and S2).

OSCC cells with Crb3 knock-down exhibit decreased cell motility. Because Crb3 is involved in colon adenocarcinoma cell migration and metastasis, Crb3 function in OSCC cell migration was investigated by siRNA-based knock-down (KD) of *Crb3*. *Crb3* expression in Ca9-22 and HSC-2 cells was knocked down using two siRNAs (siCrb3-1 and siCrb3-2) that target different sites on the *Crb3* transcript. The efficiency of knock-down by siRNAs was evaluated by detecting endogenously expressed Crb3 protein using immunoblotting (Fig. 2C and F). Ca9-22 cells treated with siCrb3-1 or siCrb3-2 displayed 92 and 75% reduction in cell motility, respectively, compared to control siRNA-treated cells (Figs. 2D and S3A). Similarly, HSC-2 cells treated with siRNAs showed 65% and 55% reduction compared to controls (Figs. 2G and S3B). Although the small difference in proliferation of siCrb3-2 treated Ca9-22 cells was observed at 96 h (Fig. 2E), siCrb3-1 treated cells did not show such difference. The proliferation was not significantly affected by knocking down *Crb3* in HSC-2 cells (Fig. 2H).

Knockout of Crb3 affects both cell motility and proliferation in OSCC cells. To assess whether the siRNA experimental results were due to off-target effects, *Crb3*-KO cell clones were established using the CRISPR-Cas9 system. *Crb3*-KO clones derived from Ca9-22 or HSC-2 were isolated by serial dilution. The deficiency of Crb3 protein in *Crb3*-KO clones of Ca9-22 (Fig. 3A) or HSC-2 (Fig. 3E) was confirmed by immunoblotting. The motility of parent and *Crb3*-KO clones of OSCC cell lines was examined by a Transwell cell migration assay. Compared to parent Ca9-22 cells, *Crb3*-KO clones (CKO#1 and CKO#2) exhibited 60 and 97% reduction in cell migration (Figs. 3B and S3C). Similarly, *Crb3*-KO clones (HKO#1 and HKO#2) showed more than 90% reduction in migration compared to parent HSC-2 cells (Figs. 3F and S3D). However, unlike *Crb3*-KD cells, the proliferation of *Crb3*-KO OSCC clones was slightly suppressed (CKO#1: 29%, CKO#2: 36%, HKO#1: 28%, HKO#2: 28%) compared to that of the respective parent cells (Fig. 3C and G). To investigate whether Crb3 promotes migration via the epithelial-mesenchymal transition (EMT) mechanism in OSCC cells, the expression of EMT markers was evaluated. Immunoblotting revealed that E-cadherin was expressed in both parent and *Crb3*-KO cells at different expression levels. In addition, the expression of EMT inducer snail family transcriptional repressor-2 (SNAI2) was not dramatically altered in *Crb3*-KO cells compared to parent cells for either cell line (Fig. 3D and H).

Crb3-KO OSCC cells show a significant reduction of lung metastases. The metastatic potentials of parent and *Crb3*-KO cells were evaluated using a xenograft model of hematogenous lung metastases (Fig. 4). Parent or *Crb3*-KO HSC-2 cells were injected into the tail veins of SCID Hairless Outbred (SHO-*Prkdc*^{scid} *Hr*^{hr}) mice. As a result, no metastases were observed in *Crb3*-KO HSC-2 cell-injected mice during the study period (n=3), whereas parent cell-injected mice developed multiple metastases in the lungs (n=3). These results indicate that Crb3 plays a key role in OSCC metastasis to the lung.

RhoA activation contributes to OSCC cell migration and proliferation. Rhosin is a small molecule inhibitor of RhoA activation. Rhosin contacts RhoA within the GEF-binding pocket, in proximity to tryptophan 58 of RhoA, to block the interaction of general Rho-GEFs with RhoA (29). To investigate whether the RhoA pathway is involved in the malignant behavior of OSCC, cell proliferation was analyzed by MTT assay using unmodified Ca9-22 or HSC-2 cells. Cell proliferation of both cell lines was partially inhibited in the presence of higher concentrations of Rhosin (Fig. 5A and E). Y16, another inhibitor of RhoA activation, specifically blocks the

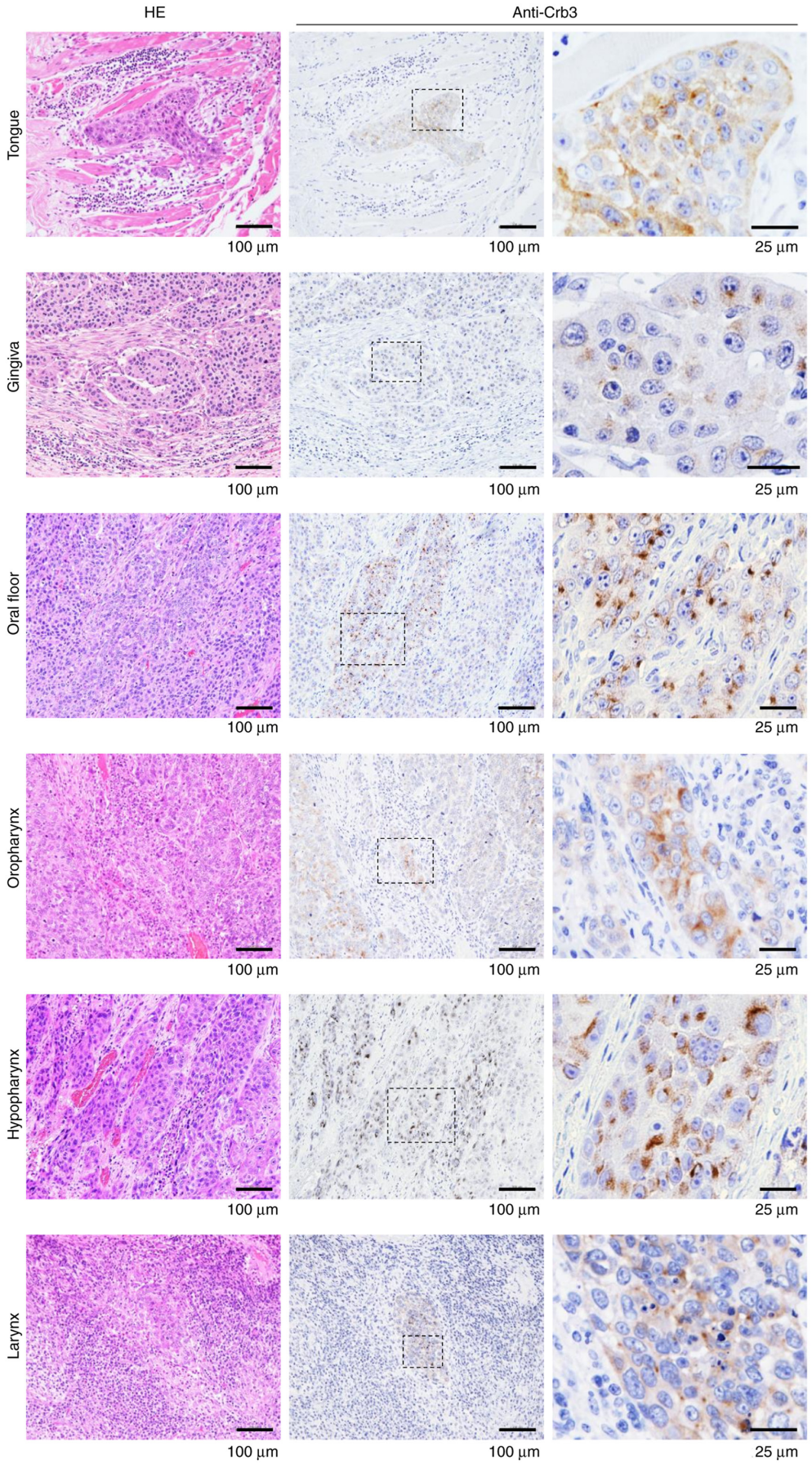

Figure 1. Crb3 is widely expressed in tissues from patients with head and neck squamous cell carcinoma. Immunohistochemical analyses were performed using squamous cell carcinoma tissues of the head and neck region, including the tongue, gingiva, oral floor, oropharynx, hypopharynx and larynx. Left panels display HE staining. Center panels indicate immunohistochemistry using an anti-Crb3 antibody with hematoxylin counterstaining. Right panels show higher magnification images of the dashed-line squares in the center panels. Crb3, crumbs3.

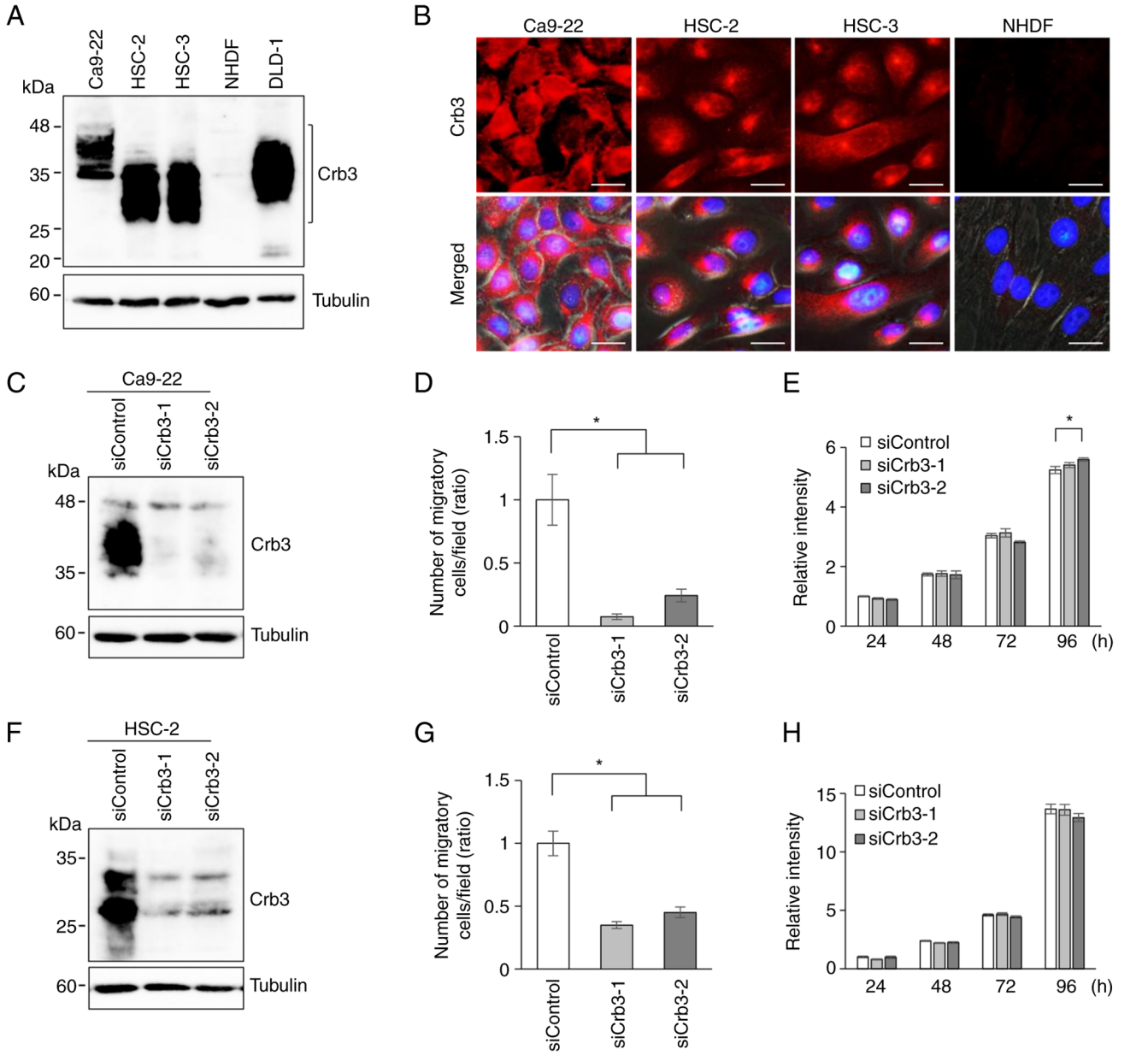

Figure 2. Knockdown of Crb3 suppresses motility in OSCC cells. (A) Crb3 expression in cells was evaluated by immunoblotting. Cell lysates from NHDF and the DLD-1 colon adenocarcinoma cell line were used as negative and positive controls, respectively. (B) Subcellular localization of Crb3 (red) in OSCC cell lines was analyzed by immunofluorescence. Cells were counterstained with Hoechst 33342. Bottom panels indicate Crb3 staining merged with Hoechst 33342 (blue) and phase contrast. Scale bar, 20 μm. Crb3 protein expression in (C) Ca9-22 or (F) HSC-2 cells treated with siRNAs was evaluated by immunoblots. Motility of (D) Ca9-22 or (G) HSC-2 cells treated with siRNAs was examined by Transwell migration assays. Proliferation of (E) Ca9-22 or (H) HSC-2 cells treated with siRNAs was assessed by MTT assays. Asterisks indicate statistically significant differences ($^*P<0.01$). Crb3, crumbs3; NHDF, normal human dermal fibroblast; OSCC, oral squamous cell carcinoma; si/siRNA, small interfering RNA.

interaction between RhoA and regulator G-protein-signaling RhoGEFs (RGS-RhoGEFs) (30). As with Rhosin, the addition of 25 μM Y16 inhibited the proliferation of Ca9-22 and HSC-2 (Fig. 5B and F). In addition, Transwell chamber assays revealed that the cell migration of Ca9-22 (Figs. 5C and S3E) and HSC-2 (Figs. 5G and S3F) was significantly inhibited in the presence of 20 μM Rhosin or 15 μM Y16 without affecting proliferation.

RhoA activation is abrogated in Crb3-KO cells. Rho-family small GTPases are major regulators of the cytoskeleton and are related to biological processes including cell migration. To address whether Crb3 affects the RhoA signaling pathway, the amount of activated RhoA in parent and *Crb3*-KO OSCC clones was examined. Endogenously expressed GTP-bound Rho-family GTPases were captured biochemically from lysates of serum-stimulated OSCC cells using rhotekin Rho-binding domain (RBD)-immobilized beads. Total cell lysates and RBD-captured samples were analyzed by immunoblotting using an anti-RhoA-specific antibody. Immunoblot analysis showed that GTP-bound RhoA is significantly depleted in *Crb3*-KO clones in both Ca9-22 and HSC-2 (Fig. 5D and H), suggesting that Crb3 functions as an upstream regulator of the RhoA pathway in OSCC cell migration.

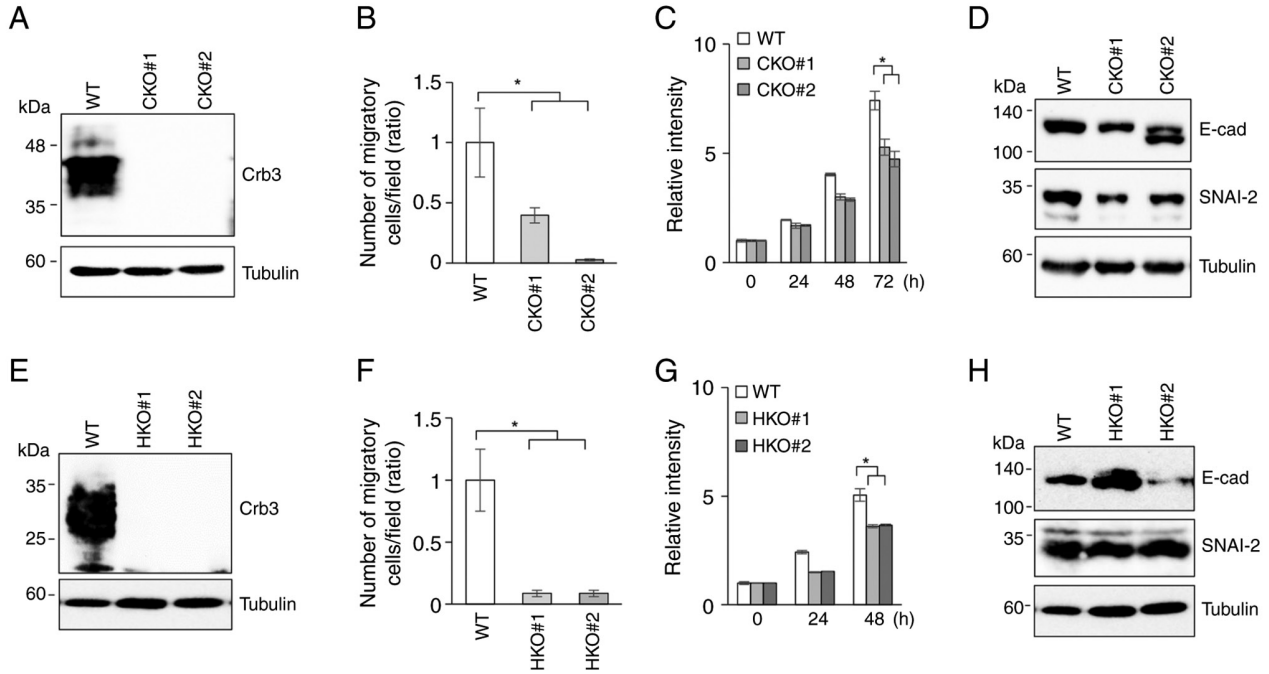

Figure 3. Knockout of *Crb3* in oral squamous cell carcinoma cells reduces cell motility without affecting EMT markers. Crb3 protein expression in *Crb3*-KO clones of (A) Ca9-22 or (E) HSC-2 cells was examined by immunoblotting. Motility of wild-type (parent) and *Crb3*-KO clones of (B) Ca9-22 or (F) HSC-2 was evaluated by Transwell migration assays. Proliferation of wild-type and *Crb3*-KO clones of (C) Ca9-22 or (G) HSC-2 was assessed using an MTT assay. EMT-related markers expressed in wild-type and *Crb3*-KO clones of (D) Ca9-22 or (H) HSC-2 were evaluated by immunoblotting. Asterisks indicate statistically significant differences (*P<0.01). Crb3, crumbs3; Crb3-KO, crumbs3-knockout; CKO, Ca9-22 *Crb3*-KO clone; E-cad, E-cadherin; EMT, epithelial-mesenchymal transition; HKO, HSC-2 *Crb3*-KO clone; SNAI-2, snail family transcriptional repressor 2; WT, wild-type.

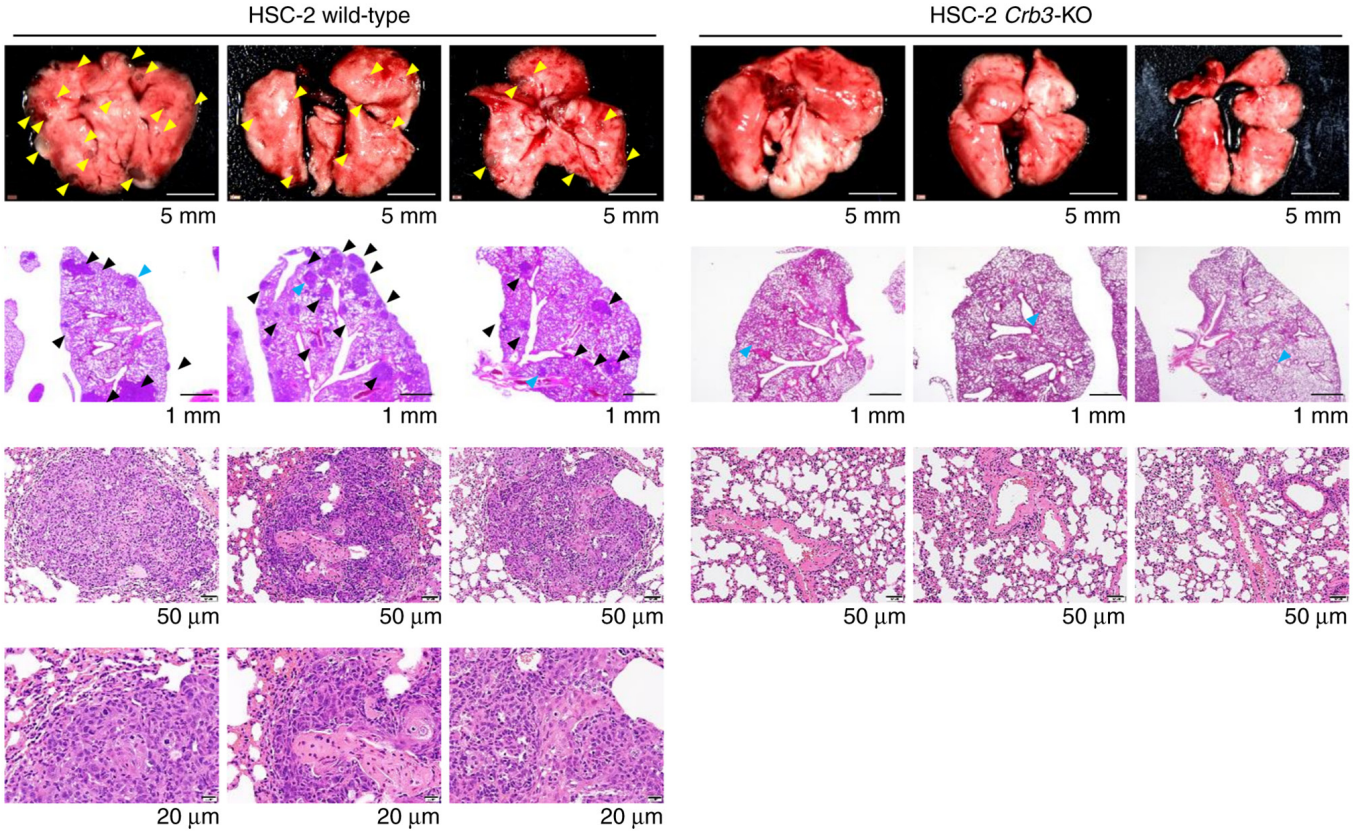

Figure 4. *Crb3*-knockout oral squamous cell carcinoma cells exhibit reduced lung metastases. Excised lungs (top panels) and HE-stained lung sections are presented. Visible metastatic tumors (yellow arrowheads) were observed on the surfaces of excised lungs from wild-type HSC-2 cell-injected mice. Low-magnification images show multiple metastatic lesions (black arrowheads) inside of the lungs from wild-type HSC-2 cell-injected mice, whereas lung metastases were not detectable in *Crb3*-KO HSC-2 cell-injected mice. Blue arrowheads indicate the regions observed at higher magnification. Crb3, crumbs3; Crb3-KO, crumbs3-knockout.

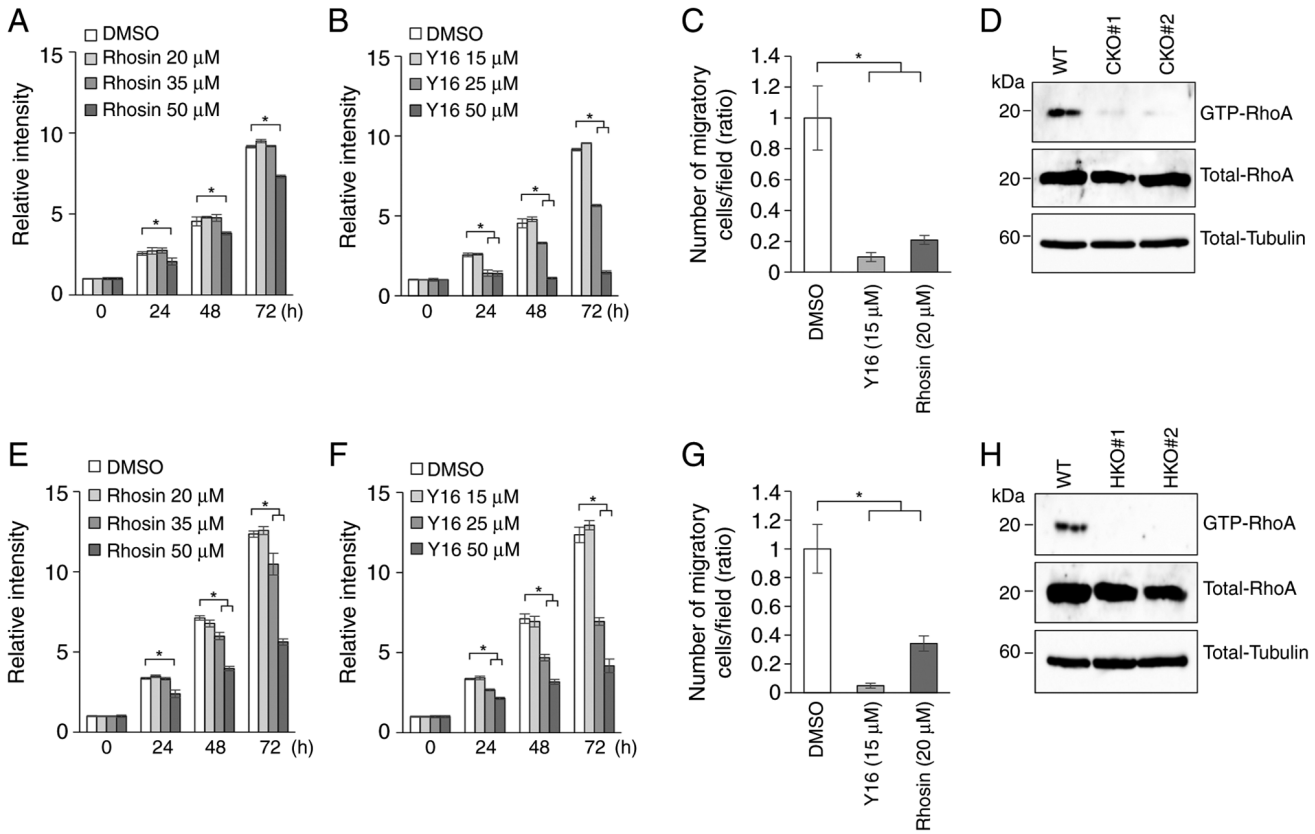

Figure 5. Crb3 promotes cell migration and proliferation by activating the RhoA pathway in oral squamous cell carcinoma cells. Proliferation of (A) Ca9-22 or (E) HSC-2 cells treated with Rhosin was analyzed by MTT assays. Proliferation of (B) Ca9-22 or (F) HSC-2 cells treated with Y16 was analyzed by MTT assays. Motility of (C) Ca9-22 or (G) HSC-2 cells treated with 15 μM Y16 or 20 μM Rhosin was examined by Transwell migration assays. Serum-induced activation of RhoA was assayed. GTP-bound RhoA expressed in wild-type and *Crb3*-KO cell clones of (D) Ca9-22 and (H) HSC-2 was isolated using recombinant RhoA binding domain of Rhotekin-conjugated beads and analyzed by immunoblotting using an anti-RhoA antibody. Asterisks indicate statistically significant differences ($^*P<0.01$). Crb3, crumbs3; Crb3-KO, crumbs3-knockout; CKO, Ca9-22 *Crb3*-KO line; DMSO, dimethyl sulfoxide; GTP, guanosine triphosphate; HKO, HSC-2 *Crb3*-KO clone; RhoA, ras homolog family member A; WT, wild-type.

Discussion

Despite advances in multimodal therapy, the long-term survival of patients with HNSCC has not been meaningfully improved. Distant metastasis is one of the major factors adversely affecting the prognosis of such patients. Finding practical diagnostic markers and developing molecular targets against tumor metastasis based on biological analysis of HNSCC are urgent issues. Our study sought to assess a novel regulatory molecule involved in malignant behaviors in OSCC, a cell type that constitutes the largest subgroup of HNSCCs (1).

Crb originally was discovered as an essential fly gene employed by *Drosophila* for ectodermal embryogenesis. Three *Crb* paralogs have been identified in the human genome, and Crb3 likely is expressed in all human epithelial cells. In a previous study, we showed that a novel monoclonal antibody raised against a C-terminal peptide unique to isoform A of human Crb3 successfully detects endogenously expressed Crb3 in colon adenocarcinomas and adjacent non-neoplastic tissues (25). However, the expression and function of Crb3 in human tissues remain poorly understood.

Immunostaining revealed that Crb3 is expressed in OSCC cell lines and tissues from patients with HNSCC. Subcellular localization of Crb3 was observed predominantly as cytoplasmic granules in most HNSCC tissues, but a diffuse staining pattern typically was observed in the cells of neighboring tissues (Fig. 1). Staining of HSC-2 and HSC-3 showed a cytoplasmic granule pattern, whereas a more diffuse pattern was observed in Ca9-22 cells (Fig. 2B). These differences in subcellular localization of Crb3 may reflect differences in the character of the originating tissues. However, tumor-adjacent non-neoplastic tissues displayed much weaker staining compared to OSCC tissues (Fig. S1). *Crb3*-KO mice exhibit severe defects in ductal epithelia in the intestine, kidney, and lung without gross anatomical defects at the body surface (23,24). These results may indicate that Crb3 is not essential for the development of the normal squamous epithelium. In contrast, the results of the present study indicated that OSCC cell migration was inhibited either by the knock-down or knock-out of *Crb3*, implying that Crb3-dependent cell migration occurs only in cancer cells in squamous epithelial tissues. EMT markers were not significantly altered by a deficiency of Crb3, suggesting that EMT is not a major downstream process by which Crb3 enhances the motility of OSCC cells. *Crb3*-KO OSCC clones were viable, albeit while displaying impaired cell growth; in contrast, knock-down of *Crb3* did not appear to affect proliferation in OSCCs. *Crb3* heterozygous mutant mice do not show apparent defects (23,24), suggesting that low-level expression of Crb3 is sufficient to drive proliferation of *Crb3*-KD cells.

The Rho family of GTPases comprises 20 members, which are involved in divergent cellular processes including cell migration and proliferation; these effects are mediated by the regulation of downstream effector molecules. The knock-down or knock-out of *RhoA* triggers compensatory changes in the expression of other *Rho* family genes; for instance, the induction of RhoB and RhoC has been reported under such conditions (31,32). To exclude the effect of compensation, analysis of the RhoA function in OSCC cell migration was demonstrated using inhibitors rather than knock-down or knock-out of *RhoA*. Specifically, 20 μM Rhosin and 15 μM Y16 were employed in assays demonstrating that the inhibition of RhoA activation affects cell migration without affecting proliferation. However, we note that exposure of cells to 50 μM Rhosin or 25 μM Y16 inhibits cell proliferation (Fig. 5A, B, E and F), suggesting that RhoA plays a bifunctional role in OSCC cells in an activity-dependent manner.

To assess whether Crb3 affects RhoA signaling, the activation of RhoA was assayed using parent cells and *Crb3*-KO clones. *Crb3*-KO clones of Ca9-22 and HSC-2 demonstrated decreased serum-induced activation of RhoA compared to that in the respective parent cells. However, RhoA activation was not decreased by knock-down of *Crb3* using siRNAs. Similarly, the proliferation of Ca9-22 and HSC-2 was not decreased significantly by knock-down of *Crb3* (Fig. 2E and H), whereas *Crb3*-KO clones exhibited impaired proliferation. These results may indicate that depletion of Crb3 by siRNA treatment is not sufficient for inactivation of RhoA and reduction of proliferation, or it may indicate that Crb3-dependent activation of RhoA is coupled to proliferation rather than cell migration in OSCC cells.

Members of the RGS-RhoGEF family of proteins, which includes LARG, PDZ-RhoGEF, and p115-RhoGEF, are regulated by the $G\alpha_{12/13}$ subunits of heterotrimeric G-proteins (33). Transwell cell migration assays indicated that the migration of OSCC cells was reduced significantly not only by the general RhoA inhibitor Rhosin but also by the RGS-RhoGEF-specific inhibitor Y16, suggesting that Crb3 affects RhoA activation in a RGS-RhoGEF-dependent manner.

There are two limitations of this study. First, the detailed molecular mechanism of RhoA activation was not clarified. The intracellular domain of Crb3 protein contains the PDZ-domain binding motif (PBM) and the FERM-domain binding motif (FBM). Intriguingly, LARG and PDZ-RhoGEF contain the PDZ-domain in their N-terminal regions. Therefore, the molecular interaction between the PBM of Crb3 and RhoGEFs should be investigated. The other limitation is that the number of samples analyzed by immunohistochemistry was still small. Although The Cancer Genome Atlas dataset of HNSCC cohorts displays no apparent correlation between *Crb3* mRNA expression and tumor malignancy or patient prognosis (data not shown), analyses of protein expression may be more appropriate to assess the clinical significance of Crb3 in HNSCC. Accordingly, further pathological investigations along with immunohistochemistry should be performed using larger tissue samples.

This study showed, for the first time (to our knowledge), that Crb3 is expressed in HNSCC patient tissues and OSCC cell lines. Additionally, functional analyses of Crb3, using knock-down or knock-out cells, demonstrated that Crb3 is involved in cell migration and proliferation, and that these effects are mediated by changes in RhoA activity in OSCC cells. These findings reveal novel aspects of Crb3 function, an insight that has potential value for the identification of molecular targets with activity against OSCC metastasis.

Acknowledgements

Not applicable.

Funding

The present study was supported by Japan Society for the Promotion of Science (JSPS) Grant-in-Aid for Scientific Research (C) (project number 20K07368), and Yamaguchi Educational and Scholarship Foundation to HI.

Availability of data and materials

The datasets used and/or analyzed during the current study are available from the corresponding author on reasonable request.

Authors' contributions

HI, AH and EK designed the project. YY and HI carried out the main experiments and data acquisition. YY and AH prepared tissue samples. EK performed pathological analyses. HI wrote the paper. HI, AH and EK supervised. YY and HI confirmed the authenticity of all the raw data. All authors read and approved the final manuscript.

Ethics approval and consent to participate

All experiments using HNSCC tissues surgically obtained from patients were approved by the Research Ethics Committee of Niigata University (approval no. #2019-0101; Niigata, Japan). Informed consent was obtained from all participants by providing an opportunity to opt-out through the website of Niigata University School of Medicine. All study procedures adhered to the principles of the Declaration of Helsinki. The animal experiments conducted in this study were approved by the Animal Care and Use Committee of Niigata University School of Medicine (approval no. SA00875; Niigata, Japan). Ethical approval was not sought for the use of primary NHDF cells in the present study.

Patient consent for publication

Not applicable.

Competing interests

The authors declare that they have no competing interests.

References

1. Sung H, Ferlay J, Siegel RL, Laversanne M, Soerjomataram I, Jemal A and Bray F: Global cancer statistics 2020: GLOBOCAN estimates of incidence and mortality worldwide for 36 cancers in 185 countries. CA Cancer J Clin 71: 209-249, 2021.

2. Johnson DE, Burtness B, Leemans CR, Lui VWY, Bauman JE and Grandis JR: Head and neck squamous cell carcinoma. Nat Rev Dis Primers 6: 92, 2020.
3. Argiris A, Karamouzis MV, Raben D and Ferris RL: Head and neck cancer. Lancet 371: 1695-1709, 2008.
4. Michiels S, Le Maître A, Buyse M, Burzykowski T, Maillard E, Bogaerts J, Vermorken JB, Budach W, PajakTF, Ang KK, *et al*: Surrogate endpoints for overall survival in locally advanced head and neck cancer: Meta-analyses of individual patient data. Lancet Oncol 10: 341-350, 2009.
5. Kuperman DI, Auethavekiat V, Adkins DR, Nussenbaum B, Collins S, Boonchalermvichian C, Trinkaus K, Chen L and MorgenszternD: Squamous cell cancer of the head and neck with distant metastasis at presentation. Head Neck 33: 714-718, 2011.
6. Liu JC, Bhayani M, Kuchta K, Galloway T and Fundakowski C: Patterns of distant metastasis in head and neck cancer at presentation: Implications for initial evaluation. Oral Oncol 88: 131-136, 2019.
7. Leibel SA, Scott CB, Mohiuddin M, Marcial VA, Coia LR, Davis LW and Fuks Z: The effect of local-regional control on distant metastatic dissemination in carcinoma of the head and neck: Results of an analysis from the RTOG head and neck database. Int J Radiat Oncol Biol Phys 21: 549-556, 1991.
8. Garavello W, Ciardo A, Spreafico R and Gaini RM: Risk factors for distant metastases in head and neck squamous cell carcinoma. Arch Otolaryngol Neck Surg 132: 762, 2006.
9. Alvi A and Johnson JT: Development of distant metastasis after treatment of advanced-stage head and neck cancer. Head Neck 19: 500-505, 1997.
10. Kotwall C, Sako K, Razack MS, Rao U, Bakamjian V and Shedd DP: Metastatic patterns in squamous cell cancer of the head and neck. Am J Surg 154: 439-442, 1987.
11. Nishijima W, Takooda S, Tokita N, Takayama S and Sakura M: Analyses of distant metastases in squamous cell carcinoma of the head and neck and lesions above the clavicle at autopsy. Arch Otolaryngol Head Neck Surg 119: 65-68, 1993.
12. Duprez F, Berwouts D, De Neve W, Bonte K, Boterberg T, Deron P, Huvenne W, Rottey S and Mareel M: Distant metastases in head and neck cancer. Head Neck 39: 1733-1743, 2017.
13. Wiegand S, Zimmermann A, Wilhelm T and Werner JA: Survival after distant metastasis in head and neck cancer. Anticancer Res 35: 5499-5502, 2015.
14. Pisani P, Airoldi M, Allais A, Valletti PA, Battista M, Benazzo M, Briatore R, Cacciola S, Cocuzza S, Colombo A, *et al*: Metastatic disease in head & neck oncology. Acta Otorhinolaryngol Ital 40 (Suppl 1): S1-S86, 2020.
15. Vega FM and Ridley AJ: Rho GTPases in cancer cell biology. FEBS Lett 582: 2093-2101, 2008.
16. Ellerbroek SM, Wennerberg K and Burridge K: Serine phosphorylation negatively regulates RhoA in vivo. J Biol Chem 278: 19023-19031, 2003.
17. Adnane J, Muro-Cacho C, Mathews L, Sebti SM and Muñoz-Antonia T: Suppression of rho B expression in invasive carcinoma from head and neck cancer patients. Clin Cancer Res 8: 2225-2232, 2002.
18. Croucher DR, Rickwood D, Tactacan CM, Musgrove EA and Daly RJ: Cortactin modulates RhoA activation and expression of Cip/Kip cyclin-dependent kinase inhibitors to promote cell cycle progression in 11q13-amplified head and neck squamous cell carcinoma cells. Mol Cell Biol 30: 5057-5070, 2010.
19. Pan Q, Bao LW, Teknos TN and Merajver SD: Targeted disruption of protein kinase Cε reduces cell invasion and motility through inactivation of RhoA and RhoC GTPases in head and neck squamous cell carcinoma. Cancer Res 66: 9379-9384, 2006.
20. Bourguignon LYW, Gilad E, Brightman A, Diedrich F and Singleton P: Hyaluronan-CD44 interaction with leukemia-associated RhoGEF and epidermal growth factor receptor promotes Rho/Ras Co-activation, phospholipase Cε-Ca^{2+} signaling, and cytoskeleton modification in head and neck squamous cell carcinoma cells. J Biol Chem 281: 14026-14040, 2006.
21. Lorenzo-Martín LF, Fernández-Parejo N, Menacho-Márquez M, Rodríguez-Fdez S, Robles-Valero J, Zumalave S, Fabbiano S, Pascual G, García-Pedrero JM, Abad A, *et al*: VAV2 signaling promotes regenerative proliferation in both cutaneous and head and neck squamous cell carcinoma. Nat Commun 11: 4788, 2020.
22. Tepass U, Theres C and Knust E: Crumbs encodes an EGF-like protein expressed on apical membranes of *Drosophila* epithelial cells and required for organization of epithelia. Cell 61: 787-799, 1990.
23. Whiteman EL, Fan S, Harder JL, Walton KD, Liu CJ, Soofi A, Fogg VC, Hershenson MB, Dressler GR, Deutsch GH, *et al*: Crumbs3 is essential for proper epithelial development and viability. Mol Cell Biol 34: 43-56, 2014.
24. Charrier LE, Loie E and Laprise P: Mouse Crumbs3 sustains epithelial tissue morphogenesis in vivo. Sci Rep 5: 17699, 2016.
25. Iioka H, Saito K, Sakaguchi M, Tachibana T, Homma K and Kondo E: Crumbs3 is a critical factor that regulates invasion and metastasis of colon adenocarcinoma via the specific interaction with FGFR1. Int J Cancer: 1-15, 2019.
26. Saito K, Mitsui A, Sumardika IW, Yokoyama Y, Sakaguchi M and Kondo E: PLOD2-driven IL-6/STAT3 signaling promotes the invasion and metastasis of oral squamous cell carcinoma via activation of integrin β1. Int J Oncol 58: 29, 2021.
27. Makarova O, Roh MH, Liu CJ, Laurinec S and Margolis B: Mammalian Crumbs3 is a small transmembrane protein linked to protein associated with Lin-7 (Pals1). Gene 302: 21-29, 2003.
28. Iioka H, Saito K and Kondo E: Crumbs3 regulates the expression of glycosphingolipids on the plasma membrane to promote colon cancer cell migration. Biochem Biophys Res Commun 519: 287-293, 2019.
29. Shang X, Marchioni F, Sipes N, Evelyn CR, Jerabek-Willemsen M, Duhr S, Seibel W, Wortman M and Zheng Y: Rational design of small molecule inhibitors targeting RhoA subfamily Rho GTPases. Chem Biol 19: 699-710, 2012.
30. Shang X, Marchioni F, Evelyn CR, Sipes N, Zhou X, Seibel W, Wortman M and Zheng Y: Small-molecule inhibitors targeting G-protein-coupled Rho guanine nucleotide exchange factors. Proc Natl Acad Sci USA 110: 3155-3160, 2013.
31. Simpson KJ, Dugan AS and Mercurio AM: Functional analysis of the contribution of RhoA and RhoC GTPases to invasive breast carcinoma. Cancer Res 64: 8694-8701, 2004.
32. Jackson B, Peyrollier K, Pedersen E, Basse A, Karlsson R, Wang Z, Lefever T, Ochsenbein AM, Schmidt G, Aktories K, *et al*: RhoA is dispensable for skin development, but crucial for contraction and directed migration of keratinocytes. Mol Biol Cell 22: 593-605, 2011.
33. Fukuhara S, Chikumi H and Gutkind JS: RGS-containing RhoGEFs: The missing link between transforming G proteins and Rho? Oncogene 20: 1661-1668, 2001.